

Recalculation of QCD Corrections to $b \rightarrow s\gamma$ Decay

Chong-Shong Gao^{a,b,c}, Jing-Liang Hu^{a,b}, Cai-Dian Lü^{a,b,c*}, Zhao-Ming Qiu^d

a CCAST(World Laboratory), P.O.Box 8730, Beijing 100080, China

b Physics Department, Peking University, Beijing 100871, China

c Institute of Theoretical Physics, Academia Sinica,

P.O.Box 2735, Beijing 100080, China

d General Office, Chinese Academy of Sciences

11 October 1993

Abstract

We give a more complete calculation of $b \rightarrow s\gamma$ decay, including leading log QCD corrections from m_{top} to M_W in addition to corrections from M_W to m_b . We have included the full set of dimension-6 operators and corrected numerical mistakes of anomalous dimensions in a previous paper[14]. Comparing with the calculations without QCD running from m_{top} to M_W [12], the inclusive decay rate is found to be enhanced. At $m_t = 150\text{GeV}$, it results in 12% enhancement, and for $m_t = 250\text{GeV}$, 15% is found. The total QCD effect makes an enhanced factor of 4.2 at $m_t = 150\text{GeV}$, and 3.2 for $m_t = 250\text{GeV}$.

PACS numbers: 12.38.Bx, 13.40.Hq, 13.20.Jf

*E-mail: lucd@itp.ac.cn

1 Introduction

Recently the CLEO collaboration has observed[1] the exclusive decay $B \rightarrow K^* \gamma$ with a branching fraction of $(4.5 \pm 1.5 \pm 0.9) \times 10^{-5}$. A new upper limit on the inclusive $b \rightarrow s\gamma$ process is also obtained as $B(b \rightarrow s\gamma) < 5.4 \times 10^{-4}$ at 95% C.L.[2]. This has been a subject of many papers[3, 4, 5, 6, 7, 8] recently. It has been argued that this experiment provides more information about restrictions on the Standard Model, Supersymmetry, Technicolor etc. Their results are found to be sensitive to the theoretical calculation of $b \rightarrow s\gamma$ decay. In order to reduce the theoretical uncertainty, a more accurate calculation of this decay rate is needed.

The radiative b quark decay has already been calculated in several papers[9]–[12]. It is found to be strongly QCD-enhanced (e.g. a factor of 7 for $m_t = 80$ GeV and $\Lambda_{QCD} = 300$ MeV in ref.[12]). In other words, the strong interaction plays an important role in this decay. However, there are still some uncertainties in these papers. In ref.[9], the anomalous dimension matrix was truncated and the estimated uncertainty due to this truncation is less than 15%. Refs.[10, 11] did not contain a full leading logarithmic analysis either, although they included some of the terms neglected in ref.[9].¹ Ref.[12] is believed to be a more accurate result. But it did not include the QCD running from m_{top} to M_W . Since the top quark is found to be heavier than W boson($m_{top} = 174 \pm 10^{+13}_{-12}$ GeV.[13]), a detailed calculation of this effect is needed . Ref.[14] does include this running, however there are some errors in the calculation of anomalous dimensions, which can lead to some changes in the final result.

In the present paper, we recalculate the $b \rightarrow s\gamma$ decay including QCD running from m_{top} to M_W , and correct the errors in ref.[14], i.e. its anomalous dimension matrix. Furthermore, we use untruncated anomalous dimensions of QCD running from M_W to m_b .

2 Matching at $\mu = m_t$

In Minimal Standard Model, we first integrate out the top quark, generating an effective five-quark theory. By using the renormalization group equation, we run the effective field theory

¹ See discussions in ref.[12].

down to the W-scale, at which the weak bosons are removed. Finally we continue running the effective field theory down to b-quark scale to calculate the rate of radiative b decay. To maintain gauge invariance, we work in a background field gauge[15].

The charged sector of Standard Model Lagrangian is

$$\begin{aligned}
\mathcal{L}_{CC} = & \frac{1}{\sqrt{2}} \mu^{\epsilon/2} g_2 \left(\bar{u} \ \bar{c} \ \bar{t} \right)_L \gamma_\mu V \begin{pmatrix} d \\ s \\ b \end{pmatrix}_L W_+^\mu \\
& + \frac{1}{\sqrt{2}} \frac{\mu^{\epsilon/2} g_2}{M_W} \left[\left(\bar{u} \ \bar{c} \ \bar{t} \right)_R M_U V \begin{pmatrix} d \\ s \\ b \end{pmatrix}_L - \left(\bar{u} \ \bar{c} \ \bar{t} \right)_L V M_D \begin{pmatrix} d \\ s \\ b \end{pmatrix}_R \right] \phi_+ \\
& + h.c..
\end{aligned} \tag{1}$$

Where V represents the 3×3 unitary Kobayashi-Maskawa matrix, M_U and M_D denote the diagonalized quark mass matrices, the subscript L and R denote left-handed and right-handed quarks, respectively.

We first integrate out the top quark, introducing dimension-6 operators to include effects of the absent top quark. In ref.[14], an approximation was made to keep only leading order terms of $\delta = M_W^2/m_t^2$, neglecting the next to leading order charged current to W boson. To include the full set of dimension-6 operators, we have to pick up five more operators involving W bosons. Our operators now make a complete basis of dimension-6 operators. Higher dimension operators are suppressed by factor p^2/m_t^2 , where p^2 characterizing the external momentum of b quark etc. $p^2 \sim m_b^2$. The basis operators are:

$$\begin{aligned}
O_{LR}^1 &= -\frac{1}{16\pi^2} m_b \bar{s}_L D^2 b_R, \\
O_{LR}^2 &= \mu^{\epsilon/2} \frac{g_3}{16\pi^2} m_b \bar{s}_L \sigma^{\mu\nu} X^a b_R G_{\mu\nu}^a, \\
O_{LR}^3 &= \mu^{\epsilon/2} \frac{e Q_b}{16\pi^2} m_b \bar{s}_L \sigma^{\mu\nu} b_R F_{\mu\nu}, \\
Q_{LR} &= \mu^\epsilon g_3^2 m_b \phi_+ \phi_- \bar{s}_L b_R, \\
P_L^{1,A} &= -\frac{i}{16\pi^2} \bar{s}_L T_{\mu\nu\sigma}^A D^\mu D^\nu D^\sigma b_L, \\
P_L^2 &= \mu^{\epsilon/2} \frac{e Q_b}{16\pi^2} \bar{s}_L \gamma^\mu b_L \partial^\nu F_{\mu\nu},
\end{aligned}$$

$$\begin{aligned}
P_L^3 &= \mu^{\epsilon/2} \frac{eQ_b}{16\pi^2} F_{\mu\nu} \bar{s}_L \gamma^\mu D^\nu b_L, \\
P_L^4 &= i\mu^{\epsilon/2} \frac{eQ_b}{16\pi^2} \tilde{F}_{\mu\nu} \bar{s}_L \gamma^\mu \gamma^5 D^\nu b_L, \\
R_L^1 &= i\mu^\epsilon g_3^2 \phi_+ \phi_- \bar{s}_L \not{D} b_L, \\
R_L^2 &= i\mu^\epsilon g_3^2 (D^\sigma \phi_+) \phi_- \bar{s}_L \gamma_\sigma b_L, \\
R_L^3 &= i\mu^\epsilon g_3^2 \phi_+ (D^\sigma \phi_-) \bar{s}_L \gamma_\sigma b_L, \\
W_{LR} &= -i\mu^\epsilon g_3^2 m_b W_+^\nu W_-^\mu \bar{s}_L \sigma_{\mu\nu} b_R, \\
W_L^1 &= i\mu^\epsilon g_3^2 W_+^\nu W_-^\mu \bar{s}_L \gamma_\mu \not{D} \gamma_\nu b_L, \\
W_L^2 &= i\mu^\epsilon g_3^2 (D^\sigma W_+^\nu) W_-^\mu \bar{s}_L \gamma_\mu \gamma_\sigma \gamma_\nu b_L, \\
W_L^3 &= i\mu^\epsilon g_3^2 W_{+\mu} W_-^\mu \bar{s}_L \not{D} b_L, \\
W_L^4 &= i\mu^\epsilon g_3^2 W_+^\nu W_-^\mu \bar{s}_L (\not{D}_\mu \gamma_\nu + \gamma_\mu \not{D}_\nu) b_L. \tag{2}
\end{aligned}$$

Where $\bar{s}_L \not{D}_\mu \gamma_\nu b_L$ stands for $\bar{s}_L D_\mu \gamma_\nu b_L + (D_\mu \bar{s}_L) \gamma_\nu b_L$ and the covariant derivative is defined as

$$D_\mu = \partial_\mu - i\mu^{\epsilon/2} g_3 X^a G_\mu^a - i\mu^{\epsilon/2} e Q A_\mu,$$

with g_3 denoting the QCD coupling constant. The tensor $T_{\mu\nu\sigma}^A$ appearing in $P_L^{1,A}$ assumes the following Lorenz structure, the index A ranging from 1 to 4:

$$\begin{aligned}
T_{\mu\nu\sigma}^1 &= g_{\mu\nu} \gamma_\sigma, & T_{\mu\nu\sigma}^2 &= g_{\mu\sigma} \gamma_\nu, \\
T_{\mu\nu\sigma}^3 &= g_{\nu\sigma} \gamma_\mu, & T_{\mu\nu\sigma}^4 &= -i\epsilon_{\mu\nu\sigma\tau} \gamma^\tau \gamma_5. \tag{3}
\end{aligned}$$

Then we can write down our effective Hamiltonian

$$\mathcal{H}_{eff} = 2\sqrt{2} G_F V_{tb} V_{ts}^* \sum_i C_i(\mu) O_i(\mu). \tag{4}$$

The matching diagrams are displayed in Fig.1 and Fig.2. The diagrams involving W bosons are introduced in addition to Goldstone boson ones, So the number of diagrams considered now is 2-times bigger than that in ref.[14]. After tedious calculation we have

$$\begin{aligned}
C_{O_{LR}^1} &= - \left(\frac{\frac{1}{2} + \frac{1}{2}\delta}{(1-\delta)^2} + \frac{\delta}{(1-\delta)^3} \log \delta \right), \\
C_{O_{LR}^2} &= - \left(\frac{\frac{1}{2}}{(1-\delta)} + \frac{\frac{1}{2}\delta}{(1-\delta)^2} \log \delta \right), \\
C_{O_{LR}^3} &= \left(\frac{1}{(1-\delta)} + \frac{\delta}{(1-\delta)^2} \log \delta \right),
\end{aligned}$$

$$\begin{aligned}
C_{P_L^{1,1}} &= C_{P_L^{1,3}} = \left(\frac{\frac{11}{18} + \frac{5}{6}\delta - \frac{2}{3}\delta^2 + \frac{2}{9}\delta^3}{(1-\delta)^3} + \frac{\delta + \delta^2 - \frac{5}{3}\delta^3 + \frac{2}{3}\delta^4}{(1-\delta)^4} \log \delta \right), \\
C_{P_L^{1,2}} &= \left(\frac{-\frac{8}{9} - \frac{1}{6}\delta + \frac{17}{6}\delta^2 - \frac{7}{9}\delta^3}{(1-\delta)^3} + \frac{-\delta + \frac{10}{3}\delta^3 - \frac{4}{3}\delta^4}{(1-\delta)^4} \log \delta \right), \\
C_{P_L^{1,4}} &= \left(\frac{\frac{1}{2} - \delta - \frac{1}{2}\delta^2 + \delta^3}{(1-\delta)^3} + \frac{\delta - 3\delta^2 + 2\delta^3}{(1-\delta)^4} \log \delta \right), \\
C_{P_L^2} &= \frac{1}{Q_b} \left(\frac{\frac{3}{4} + \frac{1}{2}\delta - \frac{7}{4}\delta^2 + \frac{1}{2}\delta^3}{(1-\delta)^3} - \frac{1}{3}\delta + \left(\frac{\frac{1}{6} + \frac{5}{6}\delta - \frac{5}{3}\delta^3 + \frac{2}{3}\delta^4}{(1-\delta)^4} - \frac{1}{6} - \frac{1}{3}\delta \right) \log \delta \right), \\
C_{P_L^3} &= 0, \\
C_{P_L^4} &= \frac{1}{Q_b} \left(\frac{-\frac{1}{2} - 5\delta + \frac{17}{2}\delta^2 - 3\delta^3}{(1-\delta)^3} + \frac{-5\delta + 7\delta^2 - 2\delta^3}{(1-\delta)^4} \log \delta + 4\delta \log \delta \right), \\
C_{R_L^1} &= C_{R_L^2} = -C_{Q_{LR}} = 1/g_3^2, \\
C_{R_L^3} &= 0, \\
C_{W_{LR}} &= C_{W_L^3} = C_{W_L^4} = 0, \\
C_{W_L^1} &= C_{W_L^2} = \delta/g_3^2. \tag{5}
\end{aligned}$$

Notice that we have included the terms of all orders of $\delta = M_W^2/m_t^2$ as far as the dimension-6 operators are concerned. However, to really achieve higher accuracy in δ , the dimension-8 operators should be considered in the matching of M_W scale². These coefficients are all from the finite part integrations of electroweak loops. Terms like $\log(\mu^2/m_t^2)$ always accompanied by the infinity $1/\epsilon$ vanishes here, because of our matching scale $\mu = m_t$. They will be regenerated by renormalization group running of electroweak in the next section.

3 Running from m_t to M_W

The renormalization group equation satisfied by the coefficient functions $C_i(\mu)$ is

$$\mu \frac{d}{d\mu} C_i(\mu) = \sum_j (\gamma^\tau)_{ij} C_j(\mu). \tag{6}$$

Where the anomalous dimension matrix γ_{ij} is calculated in practice by requiring renormalization group equations for Green functions with insertions of composite operators to be satisfied order by order in perturbation theory. Let $\Gamma_{O_i}^{(n)}$ denote a renormalized n-point 1PI Green function

²We thank Professor R. Barbieri for making this point explicit to us.

with one insertion of operator O_i . Then the anomalous dimension γ_{ij} characterizing the mixing of operator O_i into O_j is determined from the renormalization group equation for $\Gamma_{O_i}^{(n)}$,

$$\gamma_{ij} \Gamma_{O_j}^{(n)} = - \left(\mu \frac{\partial}{\partial \mu} + \beta \frac{\partial}{\partial g} + \gamma_m m \frac{\partial}{\partial m} - n \gamma_{ext} \right) \Gamma_{O_i}^{(n)}. \quad (7)$$

Here $\beta = \mu(d/d\mu)g$, $\gamma_m = (\mu/m)(d/d\mu)m$ and $n\gamma_{ext}$ stands for the wave-function anomalous dimensions arising from radiative corrections to the Green function's n external lines.

After evaluating the loop diagrams, we find the following leading order weak mixing of operators, with the Q, R part agrees with ref.[14].

$$\gamma = \begin{matrix} & O_{LR}^1 & O_{LR}^2 & O_{LR}^3 & P_L^{1,A} & P_L^2 & P_L^3 & P_L^4 \\ Q_{LR} & \left(\begin{array}{ccccccc} 0 & 0 & 0 & 0 & 0 & 0 & 0 \end{array} \right) \\ R_L^1 & \left(\begin{array}{ccccccc} 0 & 0 & 0 & 0 & 0 & 0 & 0 \end{array} \right) \\ R_L^2 & \left(\begin{array}{ccccccc} 0 & 0 & 0 & 0 & -1/2 & 0 & 0 \end{array} \right) \\ R_L^3 & \left(\begin{array}{ccccccc} 0 & 0 & 0 & 0 & 1/2 & 0 & 0 \end{array} \right) \\ W_{LR} & \left(\begin{array}{ccccccc} 0 & 0 & 6 & 0 & 0 & 0 & 0 \end{array} \right) \\ W_L^1 & \left(\begin{array}{ccccccc} 0 & 0 & 0 & 0 & 0 & 0 & 12 \end{array} \right) \\ W_L^2 & \left(\begin{array}{ccccccc} 0 & 0 & 0 & 0 & -1 & 0 & 0 \end{array} \right) \\ W_L^3 & \left(\begin{array}{ccccccc} 0 & 0 & 0 & 0 & 0 & 0 & 0 \end{array} \right) \\ W_L^4 & \left(\begin{array}{ccccccc} 0 & 0 & 0 & 0 & 0 & 0 & 0 \end{array} \right) \end{matrix} \quad 16\pi^2 \frac{g_3^2}{8\pi^2}. \quad (8)$$

These mixing are all between operators induced by tree-diagram and loop-diagram. The vanishing $\log(\mu^2/m_t^2)$ terms in the last section are regenerated here by renormalization group equation.

The QCD anomalous dimensions for each of the operators in our basis are

$$\gamma = \begin{pmatrix} O_{LR}^1 & O_{LR}^2 & O_{LR}^3 & P_L^{1,1} & P_L^{1,2} & P_L^{1,3} & P_L^{1,4} & P_L^2 & P_L^3 & P_L^4 \\ O_{LR}^1 & \frac{20}{3} & 1 & -2 & 0 & 0 & 0 & 0 & 0 & 0 \\ O_{LR}^2 & -8 & \frac{2}{3} & \frac{4}{3} & 0 & 0 & 0 & 0 & 0 & 0 \\ O_{LR}^3 & 0 & 0 & \frac{16}{3} & 0 & 0 & 0 & 0 & 0 & 0 \\ P_L^{1,1} & 6 & 2 & -1 & \frac{2}{3} & 2 & -2 & -2 & 0 & 0 \\ P_L^{1,2} & 4 & \frac{3}{2} & 0 & -\frac{113}{36} & \frac{137}{18} & -\frac{113}{36} & -\frac{4}{3} & \frac{9}{4} & 0 \\ P_L^{1,3} & 2 & 1 & 1 & -2 & 2 & \frac{2}{3} & -2 & 0 & 0 \\ P_L^{1,4} & 0 & \frac{1}{2} & 2 & -\frac{113}{36} & \frac{89}{18} & -\frac{113}{36} & \frac{4}{3} & \frac{9}{4} & 0 \\ P_L^2 & 0 & 0 & 0 & 0 & 0 & 0 & 0 & 0 & 0 \\ P_L^3 & 0 & 0 & -\frac{4}{3} & 0 & 0 & 0 & 0 & 0 & 0 \\ P_L^4 & 0 & 0 & -\frac{4}{3} & 0 & 0 & 0 & 0 & 0 & 0 \end{pmatrix} \frac{g_3^2}{8\pi^2}, \quad (9)$$

$$\gamma = \begin{pmatrix} Q_{LR} & R_L^1 & R_L^2 & R_L^3 & W_{LR} & W_L^1 & W_L^2 & W_L^3 & W_L^4 \\ Q_{LR} & \frac{23}{3} & 0 & 0 & 0 & 0 & 0 & 0 & 0 \\ R_L^1 & 0 & \frac{23}{3} & 0 & 0 & 0 & 0 & 0 & 0 \\ R_L^2 & 0 & 0 & \frac{23}{3} & 0 & 0 & 0 & 0 & 0 \\ R_L^3 & 0 & 0 & 0 & \frac{23}{3} & 0 & 0 & 0 & 0 \\ W_{LR} & 0 & 0 & 0 & 0 & 13 & 0 & 0 & 0 \\ W_L^1 & 0 & 0 & 0 & 0 & -\frac{8}{3} & \frac{23}{3} & 0 & -\frac{8}{9} \\ W_L^2 & 0 & 0 & 0 & 0 & 0 & 0 & \frac{23}{3} & 0 \\ W_L^3 & 0 & 0 & 0 & 0 & 0 & 0 & 0 & \frac{23}{3} \\ W_L^4 & 0 & 0 & 0 & 0 & 0 & 0 & 0 & -\frac{16}{9} & \frac{101}{9} \end{pmatrix} \frac{g_3^2}{8\pi^2}. \quad (10)$$

Comparing with ref.[14], except the W part, there are still some differences in the anomalous dimension matrix, which may lie in omitting a factor of 1/2 in ref.[14] in calculating Feynman diagram like Fig.3. After these changes, the whole matrix can be easily diagonalized, and all eigenvalues are real, which is required to maintain hermiticity of the effective Hamiltonian at all renormalization scales. While in ref.[14] it can not. In their case, some eigenvalues are complex.

The solution to eqn.(6) appears in obvious matrix notation as

$$C(\mu_2) = \left[\exp \int_{g_3(\mu_1)}^{g_3(\mu_2)} dg \frac{\gamma^T(g)}{\beta(g)} \right] C(\mu_1). \quad (11)$$

After inserting anomalous dimension (8–10), we can have the coefficients of operators at $\mu = M_W$. And some of these operators change a lot from ref.[14] due to our improvements. For details, see next section.

4 Matching at $\mu = M_W$

In order to continue running the basis operator coefficients down to lower scales, one must integrate out the weak gauge bosons and would-be Goldstone bosons at $\mu = M_W$ scale. The diagrams are displayed in Fig.4. In these new matching conditions, one finds the following relations between coefficient functions just above and below $\mu = M_W$:

$$\begin{aligned} C_{O_{LR}^1}(M_W^-) &= C_{O_{LR}^1}(M_W^+), \\ C_{O_{LR}^2}(M_W^-) &= C_{O_{LR}^2}(M_W^+), \\ C_{O_{LR}^3}(M_W^-) &= C_{O_{LR}^3}(M_W^+), \\ C_{P_L^{1,1}}(M_W^-) &= C_{P_L^{1,1}}(M_W^+) + 2/9, \\ C_{P_L^{1,2}}(M_W^-) &= C_{P_L^{1,2}}(M_W^+) - 7/9, \\ C_{P_L^{1,3}}(M_W^-) &= C_{P_L^{1,3}}(M_W^+) + 2/9, \\ C_{P_L^{1,4}}(M_W^-) &= C_{P_L^{1,4}}(M_W^+) + 1, \\ C_{P_L^2}(M_W^-) &= C_{P_L^2}(M_W^+) - C_{W_L^2}(M_W^+) - 3/2, \\ C_{P_L^3}(M_W^-) &= C_{P_L^3}(M_W^+), \\ C_{P_L^4}(M_W^-) &= C_{P_L^4}(M_W^+) + 9. \end{aligned} \quad (12)$$

In addition to these, there are new four-quark operators:

$$\begin{aligned} O_1 &= (\bar{c}_{L\beta} \gamma^\mu b_{L\alpha})(\bar{s}_{L\alpha} \gamma_\mu c_{L\beta}), \\ O_2 &= (\bar{c}_{L\alpha} \gamma^\mu b_{L\alpha})(\bar{s}_{L\beta} \gamma_\mu c_{L\beta}), \\ O_3 &= (\bar{s}_{L\alpha} \gamma^\mu b_{L\alpha})[(\bar{u}_{L\beta} \gamma_\mu u_{L\beta}) + \dots + (\bar{b}_{L\beta} \gamma_\mu b_{L\beta})], \end{aligned}$$

$$\begin{aligned}
O_4 &= (\bar{s}_{L\alpha}\gamma^\mu b_{L\beta})[(\bar{u}_{L\beta}\gamma_\mu u_{L\alpha}) + \dots + (\bar{b}_{L\beta}\gamma_\mu b_{L\alpha})], \\
O_5 &= (\bar{s}_{L\alpha}\gamma^\mu b_{L\alpha})[(\bar{u}_{R\beta}\gamma_\mu u_{R\beta}) + \dots + (\bar{b}_{R\beta}\gamma_\mu b_{R\beta})], \\
O_6 &= (\bar{s}_{L\alpha}\gamma^\mu b_{L\beta})[(\bar{u}_{R\beta}\gamma_\mu u_{R\alpha}) + \dots + (\bar{b}_{R\beta}\gamma_\mu b_{R\alpha})],
\end{aligned} \tag{13}$$

with coefficients

$$C_i(M_W) = 0, \quad i = 1, 3, 4, 5, 6, \quad C_2(M_W) = 1.$$

To simplify the calculation and compare with the previous results, equations of motion(EOM)[16] is used to reduce all the remaining two-quark operators to the gluon and photon magnetic moment operators O_{LR}^2 and O_{LR}^3 . The effective Hamiltonian then appears just below the W-scale as

$$\begin{aligned}
\mathcal{H}_{eff} &= \frac{4G_F}{\sqrt{2}} V_{tb} V_{ts}^* \sum_i C_i(M_W^-) O_i(M_W^-) \\
&\xrightarrow{EOM} \frac{4G_F}{\sqrt{2}} V_{tb} V_{ts}^* \left\{ \left(-\frac{1}{2} C_{O_{LR}^1} + C_{O_{LR}^2} - \frac{1}{2} C_{P_L^{1,1}} - \frac{1}{4} C_{P_L^{1,2}} + \frac{1}{4} C_{P_L^{1,4}} \right) O_{LR}^2 \right. \\
&\quad + \left(-\frac{1}{2} C_{O_{LR}^1} + C_{O_{LR}^3} - \frac{1}{2} C_{P_L^{1,1}} - \frac{1}{4} C_{P_L^{1,2}} + \frac{1}{4} C_{P_L^{1,4}} - \frac{1}{4} C_{P_L^3} - \frac{1}{4} C_{P_L^4} \right) O_{LR}^3 \\
&\quad \left. + (\text{four-quark operators}) \right\}.
\end{aligned} \tag{14}$$

For completeness, we first give the explicit expressions of the coefficient of operator O_{LR}^2 and O_{LR}^3 at $\mu = M_W^-$,

$$\begin{aligned}
C_{O_{LR}^2}(M_W^-) &= \left(\frac{\alpha_s(m_t)}{\alpha_s(M_W)} \right)^{\frac{14}{23}} \left\{ -\frac{1}{2} C_{O_{LR}^1}(m_t) + C_{O_{LR}^2}(m_t) - \frac{1}{2} C_{P_L^{1,1}}(m_t) \right. \\
&\quad \left. - \frac{1}{4} C_{P_L^{1,2}}(m_t) + \frac{1}{4} C_{P_L^{1,4}}(m_t) \right\} + \frac{1}{3},
\end{aligned} \tag{15}$$

$$\begin{aligned}
C_{O_{LR}^3}(M_W^-) &= \left(\frac{\alpha_s(m_t)}{\alpha_s(M_W)} \right)^{\frac{16}{23}} \left\{ C_{O_{LR}^3}(m_t) + 8C_{O_{LR}^2}(m_t) \left[1 - \left(\frac{\alpha_s(M_W)}{\alpha_s(m_t)} \right)^{\frac{2}{23}} \right] \right. \\
&\quad + \left[-\frac{9}{2} C_{O_{LR}^1}(m_t) - \frac{9}{2} C_{P_L^{1,1}}(m_t) - \frac{9}{4} C_{P_L^{1,2}}(m_t) + \frac{9}{4} C_{P_L^{1,4}}(m_t) \right] \left[1 - \frac{8}{9} \left(\frac{\alpha_s(M_W)}{\alpha_s(m_t)} \right)^{\frac{2}{23}} \right] \\
&\quad \left. - \frac{1}{4} C_{P_L^4}(m_t) + \frac{9}{23} 16\pi^2 C_{W_L^1}(m_t) \left[1 - \frac{\alpha_s(m_t)}{\alpha_s(M_W)} \right] \right\} - \frac{23}{12}.
\end{aligned} \tag{16}$$

They are expressed by coefficients at $\mu = m_t$ and QCD coupling α_s . So it is convenient to utilize these formula.

In the previous paper[14], the higher order terms of M_W^2/m_t^2 are included in this stage by hands in order to match the previous work[9]–[12] when $m_t \rightarrow M_W$. Therefore it is unnatural. While in this work, we keep higher order terms of M_W^2/m_t^2 from the very beginning at $\mu = m_t$ scale. If the QCD correction is ignored (by setting $\alpha_s(m_t) = \alpha_s(M_W)$ in eqn.(15),(16)), our results would reduce to the previous results[9, 12] exactly where the top quark and W bosons are integrated out together. This is required by the correctness of the effective Hamiltonian, and it is also a consistent check.

If we rewrite our operators O_{LR}^3 , O_{LR}^2 as O_7 , O_8 like ref.[12],

$$\begin{aligned} O_7 &= (e/16\pi^2)m_b\bar{s}_L\sigma^{\mu\nu}b_RF_{\mu\nu}, \\ O_8 &= (g/16\pi^2)m_b\bar{s}_L\sigma^{\mu\nu}T^ab_RG_{\mu\nu}^a. \end{aligned} \quad (17)$$

then

$$\begin{aligned} C_7(M_W) &= \frac{1}{3}C_{O_{LR}^3}(M_W^-), \\ C_8(M_W) &= -C_{O_{LR}^2}(M_W^-). \end{aligned} \quad (18)$$

The obvious differences from QCD correction to $C_7(M_W)$ and $C_8(M_W)$ can easily be seen from Fig.5 and Fig.6. In comparison to ref.[14], the enhancement of coefficient of operator O_7 is almost the same size, but the values for O_8 are quite different. Here the effect to O_8 is an enhancement rather than a suppression as in ref.[14]. At $m_t = 150\text{GeV}$, it is enhanced a factor of 40% in comparison to ref.[14]. These changes come mainly from the corrections of anomalous dimensions described earlier. Since $C_7(M_W)$ and $C_8(M_W)$ are both the input of the following QCD running from M_W to m_b , It will be is expected to change the final result.

5 The $\bar{B} \rightarrow X_s\gamma$ decay rate

The running of the coefficients of operators from $\mu = M_W$ to $\mu = m_b$ was well described in ref.[12]. After this running we have the coefficients of operators at $\mu = m_b$ scale. Table 1 gives the numerical values of coefficients of operators O_7 , O_8 with different input of top quark mass. Here we use $M_W = 80.22\text{GeV}$, $m_b = 4.9\text{GeV}$. Both $C_7(m_b)$ and $C_8(m_b)$ are enhanced in

comparison to values obtained by Misiak [12]. The obtained values of C_6 at the m_b scale are -0.030, -0.036, -0.041 for $\Lambda_{QCD}^{f=5} = 100, 200$ and 300 MeV, respectively. The corresponding values of C_5 are 0.007, 0.008 and 0.009. They are just the same as ref.[12].

The leading order $b \rightarrow s\gamma$ matrix element of H_{eff} is given by the sum of operators O_5 , O_6 and O_7 ,

$$\langle H_{eff} \rangle = -2\sqrt{2}G_F V_{ts}^* V_{tb} \{C_7(\mu) + Q_d[C_5(\mu) + 3C_6(\mu)]\} \langle |O_7| \rangle. \quad (19)$$

Therefore, the sought amplitude will be proportional to the squared modulus of

$$C_7^{eff}(m_b) = C_7(m_b) + Q_d [C_5(m_b) + 3C_6(m_b)] \quad (20)$$

instead of $|C_7(M_b)|^2$ itself.

Following ref.[9]–[12],

$$BR(\overline{B} \rightarrow X_s \gamma) / BR(\overline{B} \rightarrow X_c e \bar{\nu}) \simeq \Gamma(b \rightarrow s\gamma) / \Gamma(b \rightarrow ce\bar{\nu}). \quad (21)$$

Then applying eqs.(19),(20), one finds

$$\frac{BR(\overline{B} \rightarrow X_s \gamma)}{BR(\overline{B} \rightarrow X_c e \bar{\nu})} \simeq \frac{6\alpha_{QED}}{\pi g(m_c/m_b)} |C_7^{eff}(m_b)|^2 \left(1 - \frac{2\alpha_s(m_b)}{3\pi} f(m_c/m_b)\right)^{-1}, \quad (22)$$

where $g(m_c/m_b) \simeq 0.45$ and $f(m_c/m_b) \simeq 2.4$ corresponding to the phase space factor and the one-loop QCD correction to the semileptonic decay, respectively[17]. The electromagnetic fine structure constant evaluated at the b quark scale takes value as $\alpha_{QED}(m_b) = 1/132.7$. Afterwards one obtains the $\overline{B} \rightarrow X_s \gamma$ decay rate normalized to the quite well established semileptonic decay rate. The results are summarized in Fig.7 as functions of the top quark mass: The two upper solid lines represent the QCD-corrected ratio of the decay rates, corresponding to $\Lambda_{QCD}^{f=5} = 100$ MeV and $\Lambda_{QCD}^{f=5} = 300$ MeV, respectively. While the dashed lines correspond to the results obtained by Misiak[12]. The QCD-uncorrected values are also shown.

In this figure, we can easily see that, at $m_t = 150$ GeV, it results in 12% enhancement from Misiak's result[12], and for $m_t = 250$ GeV, 15% is found.

6 Conclusion

As a conclusion, we have given the full leading log QCD corrections(include QCD running from m_{top} to M_W), with whole anomalous dimension matrix untruncated. Comparison to the previous calculation[14], three points are improved:

- (1) We have included the full set of dimension-6 operators.
- (2) We correct errors of anomalous dimensions in ref.[14].
- (3) We use untruncated anomalous dimensions in QCD running from M_W to m_b instead of truncated ones.

In fact, point(2) makes an enhancement while point(3) leads to a suppression. For point(1) there is no significance change in final result. The total result does not change a lot, e.g. a suppression of 4% comparing ref.[14]. Table 2 gives the results by different authors.

The whole QCD-enhancement of the $BR(\bar{B} \rightarrow X_s \gamma)$ makes a factor of 4.4 at $m_t = 145\text{GeV}$, and 3.2 at $m_t = 250\text{GeV}$, when $\Lambda_{QCD} = 200\text{MeV}$.

The branching ratio $BR(\bar{B} \rightarrow X_s \gamma)/BR(\bar{B} \rightarrow X_c e\bar{\nu})$ ranges from about 3×10^{-3} to 6×10^{-3} as m_t varies from 90GeV to 250GeV($\Lambda_{QCD} = 200\text{MeV}$). Although this result is not quite different from the previous calculations, our improvements lie in reducing some theoretical uncertainties. This improvements are important, since the anomalous dimension matrix of ref.[14] is not a hermitian one, and its results are not faithful.

The gluon magnetic moment operator O_8 is also enhanced from Misiak's result[12], which is not the present paper's interest.

Acknowledgement

One of the authors(C.D. Lü) is grateful to Prof. Xiaoyuan Li for stimulating of this work and helpful discussions. We also thank Prof. Y.B. Dai, T. Huang, Y.P. Kuang, Z.X. Zhang, G.D. Chao, and Dr. Y.Q. Chen, Y. Liao, Q. Wang, Q.H. Zhang for helpful discussions. This work is partly supported by the National Natural Science Foundation of China and the Doctoral Program Foundation of Institution of Higher Education.

References

- [1] R. Ammar, et al. CLEO Collaboration, Phys. Rev. Lett. **71** (1993) 674.
- [2] E. Thorndike, CLEO Collaboration, talk given at the *1993 Meeting of the American Physical Society*, Washington, D.C., April, 1993.
- [3] J.L. Hewett, Phys. Rev. Lett. **70** (1993) 1045.
- [4] V. Barger, M.S. Berger and R.J.N. Phillips, Phys. Rev. Lett. **70** (1993) 1368.
- [5] T. Rizzo, Argonne National Laboratory report, ANL-HEP-PR-93-19, 1993.
- [6] J.L. Hewett and T. Rizzo, Argonne National Laboratory report, ANL-HEP-PR-93-37, 1993.
- [7] A. Ali and G. Greub, preprint, DESY 93-065, ZU-TH 11/19, 1993.
- [8] A.J. Buras, M. Misiak, M. Münz, S. Pokorski, Nucl. Phys. **B424** (1994) 374; and references therein.
- [9] B. Grinstein, R. Springer and M.B. Wise, Phys. Lett. **B202** (1988) 138; Nucl. Phys. **B339** (1990) 269.
- [10] R. Grigjanis, P. O'Donnell and M. Sutherland, Phys. Lett. **B213** (1988) 355; Erratum, **B286** (1992) 413.
- [11] G. Cella, G. Curci, G. Ricciardi and A. Vicere, Phys. Lett. **B248** (1990) 181.
- [12] M. Misiak, Phys. Lett. **B269** (1991) 161; Nucl. Phys. **B393** (1993) 23.
- [13] F. Abe et al. CDF Collaboration, Phys. Rev. Lett. **73** (1994) 225.
- [14] P. Cho, B. Grinstein, Nucl. Phys. **B365** (1991) 279.
- [15] L. Abbott, Nucl. Phys. **B185** (1981) 189.
- [16] H.D. Politzer, Nucl. Phys. **B172** (1980) 349; H. Simma, preprint, DESY 93-083.
- [17] N. Cabibbo and L. Maiani, Phys. Lett. **B79** (1978) 109.

Table 1: Numerical results for coefficients of operators $C_i(m_b)$.

m_{top} (GeV)	$c_7(m_b)$			$c_8(m_b)$		
	$\Lambda=100$	$\Lambda=200$	$\Lambda=300$	$\Lambda=100$	$\Lambda=200$	$\Lambda=300$
100	-0.297	-0.324	-0.345	-0.151	-0.163	-0.173
110	-0.307	-0.333	-0.353	-0.155	-0.168	-0.177
120	-0.315	-0.341	-0.361	-0.160	-0.172	-0.181
130	-0.323	-0.349	-0.368	-0.163	-0.175	-0.184
140	-0.330	-0.356	-0.375	-0.166	-0.178	-0.187
150	-0.337	-0.362	-0.381	-0.169	-0.181	-0.190
160	-0.343	-0.368	-0.387	-0.172	-0.184	-0.193
170	-0.349	-0.374	-0.393	-0.174	-0.186	-0.195
180	-0.354	-0.379	-0.398	-0.176	-0.188	-0.197
190	-0.360	-0.384	-0.402	-0.178	-0.190	-0.199
200	-0.364	-0.388	-0.407	-0.180	-0.191	-0.200
210	-0.369	-0.393	-0.411	-0.181	-0.193	-0.202
220	-0.373	-0.397	-0.415	-0.183	-0.194	-0.203
230	-0.377	-0.401	-0.419	-0.184	-0.196	-0.204
240	-0.381	-0.404	-0.422	-0.185	-0.197	-0.205
250	-0.384	-0.408	-0.426	-0.187	-0.198	-0.207

 Table 2: Enhancement(+) or suppression(−) of $b \rightarrow s\gamma$ decay rates obtained by Cho et al.[14], Misiak[12] and the present improved ones relative to earlier result by Grinstein et al.[9]

	Grinstein et al.	Cho et al.	Misiak	This paper
QCD running $M_W \rightarrow m_b$	truncated	truncated	untruncated	untruncated
QCD running $m_t \rightarrow M_W$	neglected	performed	neglected	performed
$m_{top}=150\text{GeV}$	1	+8%	-6%	+5%
$m_{top}=250\text{GeV}$	1	+14%	-5%	+10%

Figure Captions

Fig.1 Leading order matching conditions at the top quark scale for the 1PI Green functions in the full Standard Model and in the intermediate effective field theory.

Fig.2 One loop matching conditions at the top quark scale for the 1PI Green functions in the full Standard Model and in the intermediate effective field theory.

Fig.3 One of the Feynman diagram in calculating Anomalous dimensions, with the heavy dot denoting high dimension operator.

Fig.4 Matching conditions at $\mu = M_W$ for four quarks and two quarks 1PI Green functions in the intermediate effective field theory and effective field theory below W scale.

Fig.5 The photon magnetic moment operator's coefficient $C_7(M_W)$ for different top quark mass. The ones with and without QCD corrections are indicated by solid and dashed lines respectively. ($\Lambda = 300\text{MeV}$ is used)

Fig.6 The gluon magnetic moment operator's coefficient $C_8(M_W)$ for different top quark mass. The ones with and without QCD corrections are indicated by solid and dashed lines respectively. ($\Lambda = 300\text{MeV}$ is used)

Fig.7 $\text{BR}(\overline{B} \rightarrow x_s \gamma)$ normalized to $\text{BR}(\overline{B} \rightarrow x_c e \bar{\nu})$, as function of top quark mass. The upper solid lines indicated our results for a full QCD correction. Dashed lines correspond to Misiak's results without QCD running from m_{top} to M_W .

This figure "fig1-1.png" is available in "png" format from:

<http://arxiv.org/ps/hep-ph/9408351v2>

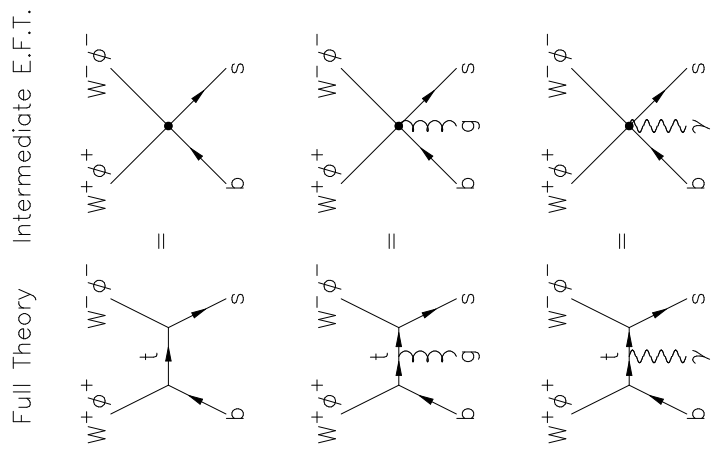


Fig. 1

This figure "fig1-2.png" is available in "png" format from:

<http://arxiv.org/ps/hep-ph/9408351v2>

Full Theory

Intermediate E.F.T.

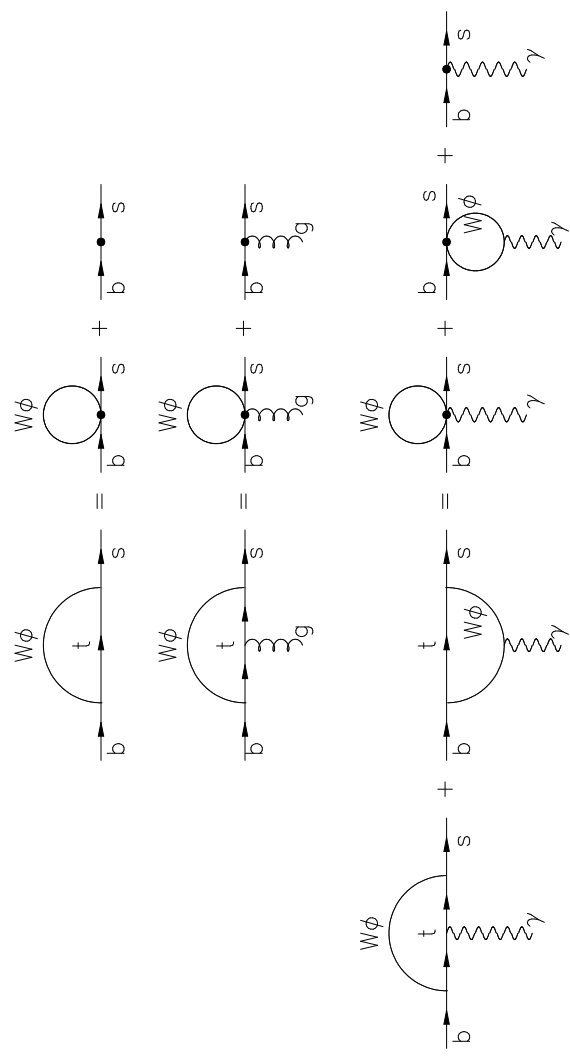


Fig. 2

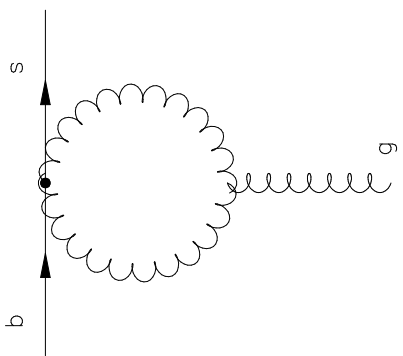


Fig. 3

Intermediate E.F.T. E.F.T. below W scale

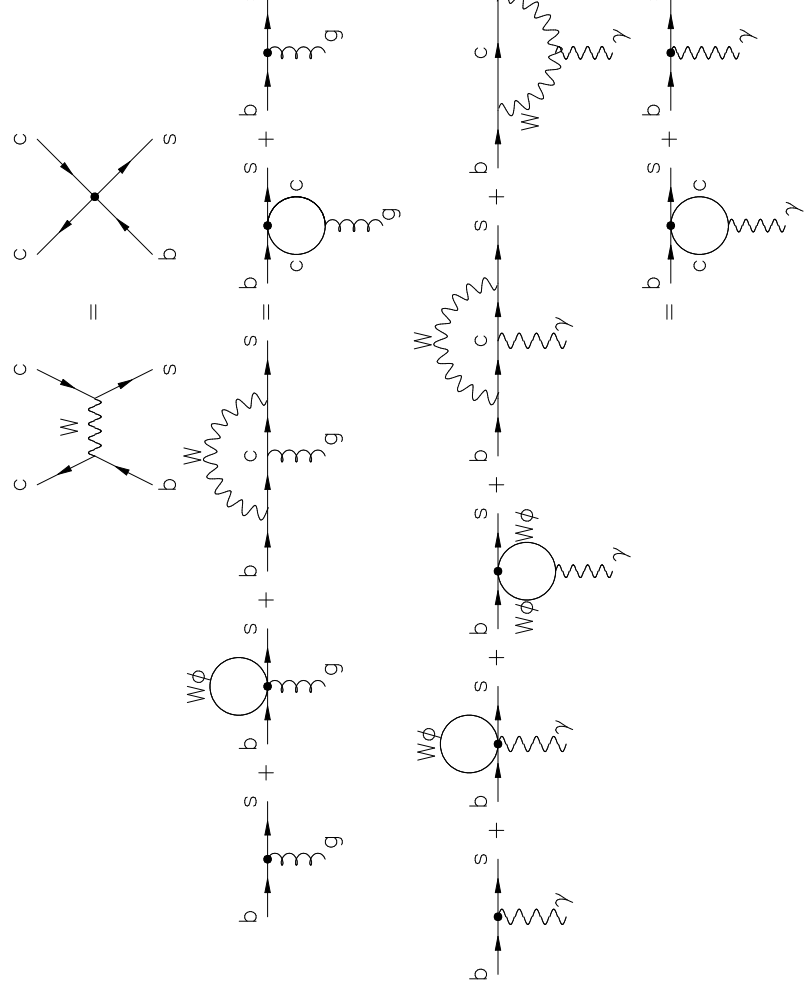


Fig. 4

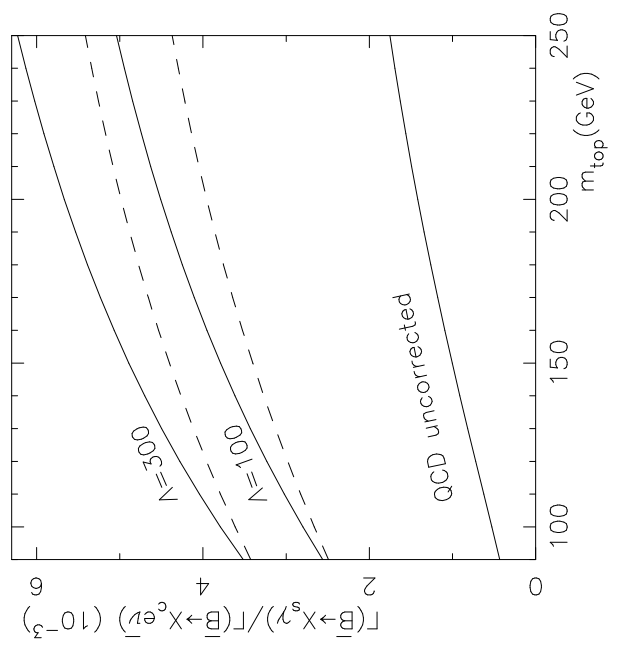


Fig. 7

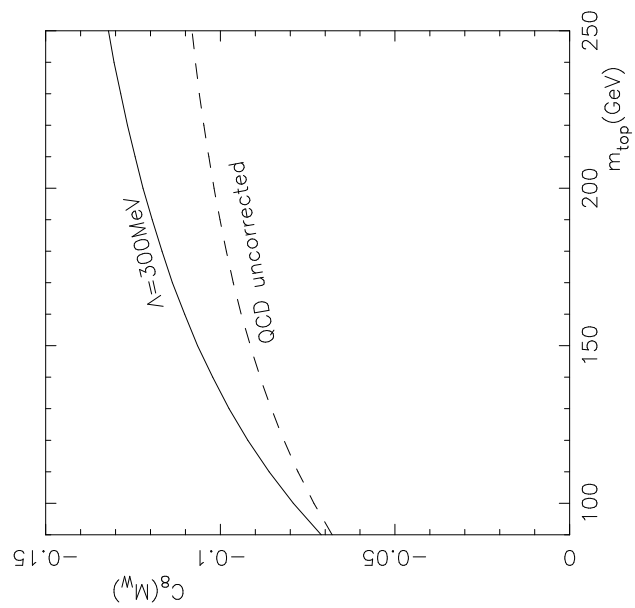


Fig. 6

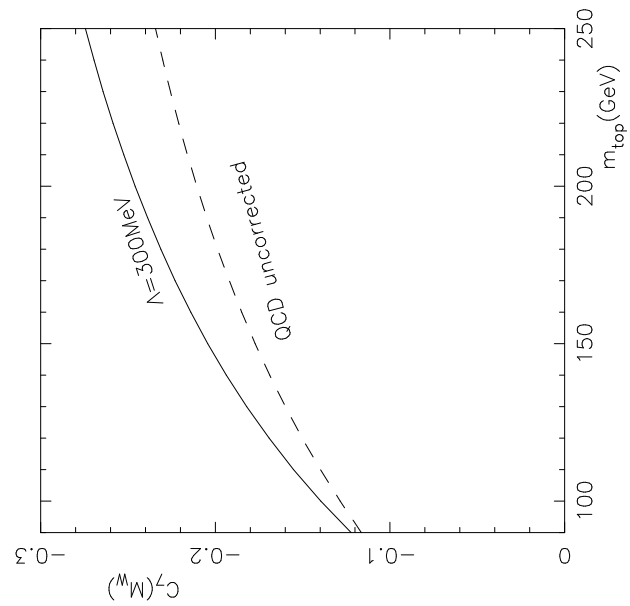


Fig. 5